AD-A139 073 DISCRETE CHARGE DIAGNOSTICS ON PRE-DIRECT COURSE(U) AIR 1/1
FORCE WEAPONS LAB KIRTLAND AFB NM R L GUICE ET AL.
FEB 84 AFWL-TR-83-51

UNCLASSIFIED F/G 19/4 NL

END
DATE FILMED
4-84
DTIC

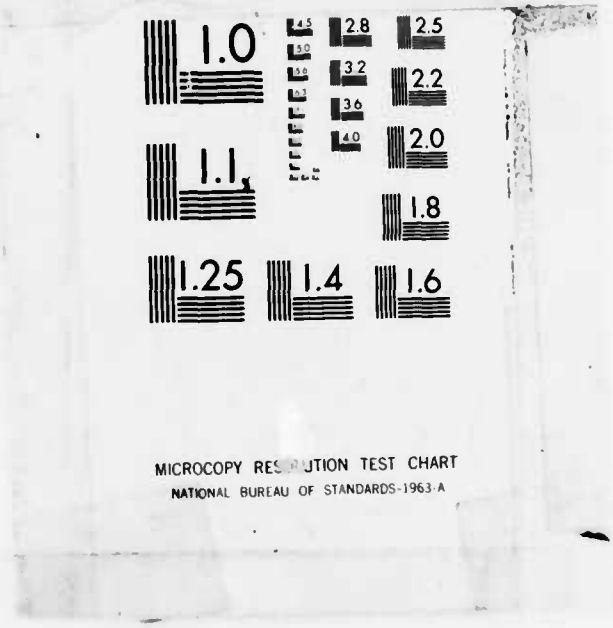
1.0
2.8
2.5
3.2
2.2
3.6
4.0
2.0
1.1
1.8
1.25
1.4
1.6
MICROCOPY RESOLUTION TEST CHART
NATIONAL BUREAU OF STANDARDS-1963-A

AD A139073

AFWL-TR-83-51

AFWL-TR-
83-51

DISCRETE CHARGE DIAGNOSTICS ON PRE-DIRECT COURSE

Robert L. Guice
Charles Bryant

February 1984

Final Report

Approved for public release; distribution unlimited.

DTIC FILE COPY

DTIC
ELECTE
MAR 1 9 1984
S
D
E

AIR FORCE WEAPONS LABORATORY
Air Force Systems Command
Kirtland Air Force Base, NM 87117

This final report was prepared by the Air Force Weapons Laboratory, Kirtland Air Force Base, New Mexico, under Job Order WDNS9217. Lieutenant Steven D. Wert (NTED) was the Laboratory Project Officer-in-Charge.

When Government drawings, specifications, or other data are used for any purpose other than in connection with a definitely Government-related procurement, the United States Government incurs no responsibility or any obligation whatsoever. The fact that the Government may have formulated or in any way supplied the said drawings, specifications, or other data, is not to be regarded by implication, or otherwise in any manner construed, as licensing the holder, or any other person or corporation; or conveying any rights or permission to manufacture, use, or sell any patented invention that may in any way be related thereto.

This report has been authored by an employee of the United States Government. Accordingly, the United States Government retains a nonexclusive, royalty-free license to publish or reproduce the material contained herein, or allow others to do so, for the United States Government purposes.

This report has been reviewed by the Public Affairs Office and is releasable to the National Technical Information Services (NTIS). At NTIS, it will be available to the general public, including foreign nations.

If your address has changed, if you wish to be removed from our mailing list, or if your organization no longer employs the addressee, please notify AFWL/NTED, Kirtland AFB, NM 87117 to help us maintain a current mailing list.

This technical report has been reviewed and is approved for publication.

STEVEN D. WERT
Lieutenant, USAF
Project Officer

FOR THE COMMANDER

T. D. McCARSON, JR
Lt Colonel, USAF
Chief, Technology Branch

JOHN H. STORM
Colonel, USAF
Chief, Civil Engineering Research Div

DO NOT RETURN COPIES OF THIS REPORT UNLESS CONTRACTUAL OBLIGATIONS OR NOTICE ON A SPECIFIC DOCUMENT REQUIRES THAT IT BE RETURNED.

UNCLASSIFIED
SECURITY CLASSIFICATION OF THIS PAGE

REPORT DOCUMENTATION PAGE

1a. REPORT SECURITY CLASSIFICATION Unclassified	1b. RESTRICTIVE MARKINGS
2a. SECURITY CLASSIFICATION AUTHORITY	3. DISTRIBUTION/AVAILABILITY OF REPORT Approved for public release; distribution unlimited.
2b. DECLASSIFICATION/DOWNGRADING SCHEDULE	
4. PERFORMING ORGANIZATION REPORT NUMBER(S) AFWL-TR-83-51	5. MONITORING ORGANIZATION REPORT NUMBER(S)
6a. NAME OF PERFORMING ORGANIZATION Air Force Weapons Laboratory 6b. OFFICE SYMBOL (If applicable) NTEDA	7a. NAME OF MONITORING ORGANIZATION Defense Nuclear Agency
6c. ADDRESS (City, State and ZIP Code) Kirtland Air Force Base, NM 87117	7b. ADDRESS (City, State and ZIP Code) Washington, DC 20305
8a. NAME OF FUNDING/SPONSORING ORGANIZATION 8b. OFFICE SYMBOL (If applicable)	9. PROCUREMENT INSTRUMENT IDENTIFICATION NUMBER
8c. ADDRESS (City, State and ZIP Code)	10. SOURCE OF FUNDING NOS. PROGRAM ELEMENT NO.: 62715H; PROJECT NO.: WDNS; TASK NO.: 92; WORK UNIT NO.: 17
11. TITLE (Include Security Classification) DISCRETE CHARGE DIAGNOSTICS ON PRE-DIRECT COURSE	
12. PERSONAL AUTHOR(S) Robert L. Guice and Charles Bryant	
13a. TYPE OF REPORT Final Report 13b. TIME COVERED FROM Jan 82 TO Dec 82	14. DATE OF REPORT (Yr., Mo., Day) 1984 February 15. PAGE COUNT 41
16. SUPPLEMENTARY NOTATION This research was sponsored by the Defense Nuclear Agency under Subtask H42BAXYX; Work Unit 0010; Work Unit Title, General Support Work.	
17. COSATI CODES FIELD: 19; GROUP: 04; SUB. GR.	18. SUBJECT TERMS (Continue on reverse if necessary and identify by block number) High Explosives, Digital Measurements, Shock Time of Arrival, ANFO, Pre-DIRECT COURSE

19. ABSTRACT (Continue on reverse if necessary and identify by block number)

The Air Force Weapons Laboratory attempted to make 100 time-of-arrival measurements on Pre-DIRECT COURSE. With an 88 percent success rate, the detonation wave propagation within the charge was measured. The top and bottom hemispheres detonated at two different rates. However, the detonation velocities were well within the existing data base for Ammonium-Nitrate Fuel Oil charges. One large jet was observed on the charge but its location should not have caused any problems for ground level measurements.

Twenty experimental time-of-arrival crystals were also fielded; however, the results are skeptical due to the grounding system of the support structure.

20. DISTRIBUTION/AVAILABILITY OF ABSTRACT UNCLASSIFIED/UNLIMITED ☐ SAME AS RPT. ☒ OTIC USERS ☐	21. ABSTRACT SECURITY CLASSIFICATION Unclassified
22a. NAME OF RESPONSIBLE INDIVIDUAL Lt Steven D. Wert	22b. TELEPHONE NUMBER (Include Area Code) (505) 844-0262 22c. OFFICE SYMBOL NTEDA

DD FORM 1473, 83 APR EDITION OF 1 JAN 73 IS OBSOLETE.

UNCLASSIFIED
SECURITY CLASSIFICATION OF THIS PAGE

PREFACE

The authors would like to record their appreciation to A1C Jeffery Slopek and Thomas Young (AFWL/NTEO) for their assistance in instrumentation work in the field. In addition we wish to thank Messrs Bruce Schneider, Paul Reining, Ruel Thompson, and Curtis Burnett of New Mexico Engineering Research Institute for their assistance in field installation of the time of arrival crystals. We would also like to thank Mses Jeannine Nelson and Donese Jones for their help with data reduction and Mmes Betty Iiames and Lori McCardle for their help in report preparation.

CONTENTS

ILLUSTRATIONS

TABLES

I. TIME OF ARRIVAL DATA SYSTEM

1. INTRODUCTION

The Air Force Weapons Laboratory (AFWL) was asked by Field Command Defense Nuclear Agency to determine the charge burn rate and symmetry on the Pre-DIRECT COURSE test. The AFWL fielded two units of a Time of Arrival Data System (TOADS) to make 120 discrete measurements. Eighty of the TOA detectors were implanted in the Ammonium Nitrate Fuel Oil (ANFO) explosive on known radials and distances from the center of the sphere. Two additional detectors were attached to the booster to determine ANFO ignition time. An additional 18 detectors were fixed on the outer skin of the fiberglass sphere to determine true charge breakout. Twenty experimental modified TOA detectors were installed on the ground, 23 m from ground zero.

2. TOADS

The TOADS is built upon a stopwatch principle. It has a measurement clock, a start-stop gage, the acquisition device, a memory, the display, and the power supply, all in one small unit. The AFWL TOADS is a digital concept which moves the data storage into a digital memory in a forward location. It produces the measurement there, as opposed to obtaining the results from an analog tape, and transmits all 100 measurements of a forward system over one inexpensive, twisted pair cable to the instrumentation van for printing.

The principal organization of the TOADS is shown in more detail in Figure 1. A piezotransducer (crystal) supplies the stop signal to the counter (that was started at time zero) by gating the count pulses in the forward controller onto a count bus. The information contained in the counter, is the elapsed time from time zero to the arrival of the event at this station. It is held there in a memory, channel by channel, for safekeeping until it can be read out. Each channel is identified by a unique number that is also used for requesting the channel information for readout. The forward system is battery operated and independent of main power.

The forward controller can exercise fully the whole forward system except for printing. It provides the clocks, receiver and transmitter circuits, and several diagnostic tests that are designed to check out the system operation. Channels can be addressed individually for data readout, channel status, and

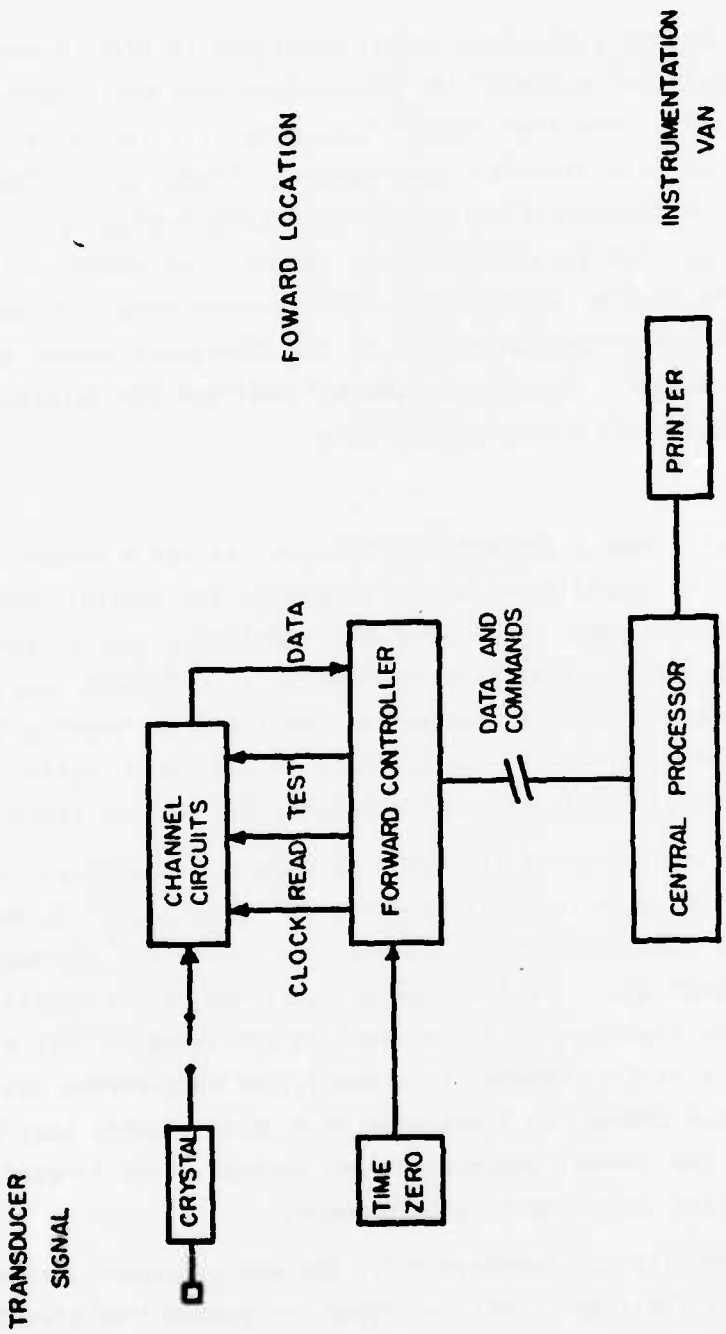

Figure 1. AFWL digital TOAD system.

error flags which are displayed on the front panel. Upon request from the central processor, data, status, and errors are transmitted to the instrumentation van for printing or display.

In the central processor, controls are the same as in the forward controller. Address indexing for automatic printout of the whole system and the control over data transmissions is unique to the processor. The printer is the only peripheral. It prints the arrival times in milli- or microseconds, identifies the channel by a three-digit number, two digits for the channel and one digit for the system number of a 10-forward system complement, and prints the errors that have occurred in connection with a measurement.

The measurement range has been laid out for six-decimal digits. This allows a maximum time of 100 ms to be accumulated with a resolution of 0.2 μs. The design of the high frequency circuits provides for a response of 35 MHz. The master clock is in the forward controller. With clock rate divisions of 5 and then 10, lower resolutions of 1, 10, and 100 μs, and 1, 10, and 100 ms can be obtained, resulting in total time accumulation of 1, 10, 100 ms, and 1, 10, and 100 s, respectively. An external clock can be used for other values.

The total error of a measurement consists of the constant error and a proportional error. The constant error is the resolution which is ±0.2 μs in the highest range. The proportional error results from the accuracy of the master clock. An oscillator with 1 ppm accuracy is postulated in this discussion. This means that for a counter range of 100 ms, the deviation from absolute time is ±0.1 μs (at the 10 MHz clock rate). Because this is a time proportional error, it is only 10 ns for a reading of 10 ms which is representative for most of the tests done. Including a temperature error of ±5 ppm for the range from 273 to 323 K and adding other effects for good measure, not more than ±0.1 μs proportional error has to be added to the constant error, resulting in a total error of ±0.3 μs for readings in the 10s of ms.

3. TOA DETECTOR PLACEMENT

The two piezoelectric crystals on the octol booster were attached by tape to the charge. They were on a plane through the center of the booster, 90 deg from the detonator access hole. The crystals, cables, and booster were

inserted into the ANFO volume when the sphere was half filled. The cables then exited the sphere through the top, to be connected at a later time.

The 80 piezoelectric crystals located on radials throughout the ANFO were attached to 0.47 cm (0.185 in) diameter cotton rope. The rope was attached to a 0.63 cm (0.25 in) thick fiberglass ring on the exterior of the center fiberglass column and the opposite end was tied to a 0.63 cm (0.25 in) thick pine wood block bolted to the fiberglass sphere. This type of installation allowed for sufficient tension in the rope to minimize position uncertainty during the ANFO loading operation. Also by using the fiberglass rings as an attachment point, the radials can be extrapolated to the center of the sphere without surrendering exact distances. The cables from the crystals were routed along the rope to a 1.27 cm (0.5 in) diameter exit hole in the sphere. This method of cable routing was favored due to the perceived burn characteristics of the spherical charge; i.e., the most interior crystals would be triggered before the next distant crystals, etc.

The 18 exterior crystals were attached to the measured locations on the fiberglass sphere by duct tape. This simple method produces an adequate low-cost bond. The cables from these crystals were routed along the exterior of the sphere to various *guy* cables.

Cable position is an important yet low priority criterion for a test of this geometry. It is assumed, and hoped, that the charge will burn with perfect symmetry; however, this is usually not the result. In almost every ANFO field test to date some type of burn inequality has occurred; this leads to a conservative design outlook. On Pre-DIRECT COURSE the cables attached to the piezoelectric crystals were draped and crossed over the sphere's surface in such a manner to minimize cable damage if a jet was formed during detonation. The cables were then led down two of the tower's guy cables and back to the forward controller, via a shallow trench.

4. TOA CRYSTAL LOCATIONS

As previously mentioned, the piezoelectric crystals were placed on various radials throughout the charge and on the surface of the container. Figure 2 shows typical crystal radials and locations in the interior and exterior of the charge.

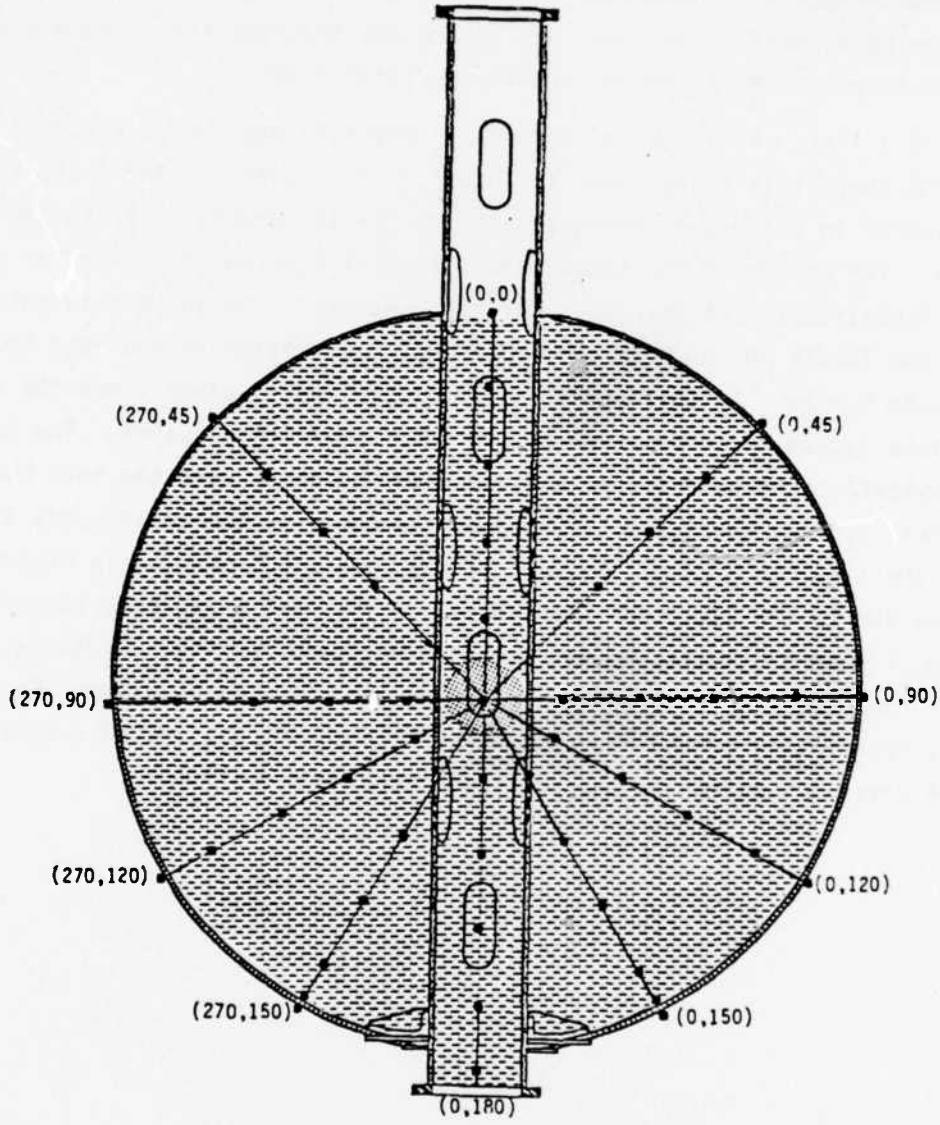

Figure 2. Typical TOA location.

Since all of the other measurements were near the ground surface, it was felt that the bottom hemisphere of the charge would highly influence the ground measurements. Therefore, 77 percent of the crystals were located in the lower hemisphere. The upper hemisphere was instrumented in such a fashion as to be able to make a comment about detonation symmetry.

Table 1 lists all of the piezoelectric crystal locations. Figure 3 presents the coordinate system used in locating the crystals. The X and Y axes are parallel to the ground surface with the Z-axis perpendicular to the same surface. The center of the coordinate system is located at the center of the sphere (specifically at the center of the booster). The angle Θ is measured around the Z-axis which would measure a location similar to the test bed coordinate system. At this point a word of caution is given since the crystal coordinate system is in relation to the tower coordinate system. The tower (and crystal) coordinate system is 15 deg out of phase with the test bed coordinate system, specifically 0 deg on the tower system corresponds to 15 deg on the test bed system. Angle Φ is measured about the Y-axis clockwise from the top to the bottom of the sphere. Given that Θ can vary between 0 and 360 deg, Φ must be limited to a range between 0 and 180 deg. Distance is measured as a vector, R, from the center of the coordinate system. Appendix A gives a description of the raw test data. The column designated ε relates the TOA crystal location to the test bed coordinate system.

TABLE 1. TOA LOCATIONS

RADIAL NUMBER	Θ (degrees)	Φ (degrees)	DISTANCE (meters) 0.38	0.76	1.14	1.52	1.77	1.84
1	0	0	X	X	X	X	X	X
2	0	45		X	X	X		X
3	0	90	X	X	X	X		X
4	0	120	X	X	X	X		X
5	0	150		X	X	X	X	X
6	0	180	X	X	X	X		X
7	45	135		X	X	X		
8	90	45		X	X	X		X
9	90	90	X	X	X	X		X
10	90	120	X	X	X	X		X
11	90	150		X	X	X	X	X
12	135	135		X	X	X		
13	180	45		X	X	X		X
14	180	90	X	X	X	X		X
15	180	120	X	X	X	X		X
16	180	150		X	X	X	X	X
17	225	135		X	X	X		
18	270	45		X	X	X		X
19	270	90	X	X	X	X		X
20	270	120	X	X	X	X		X
21	270	150		X	X	X	X	X
22	315	135		X	X	X		

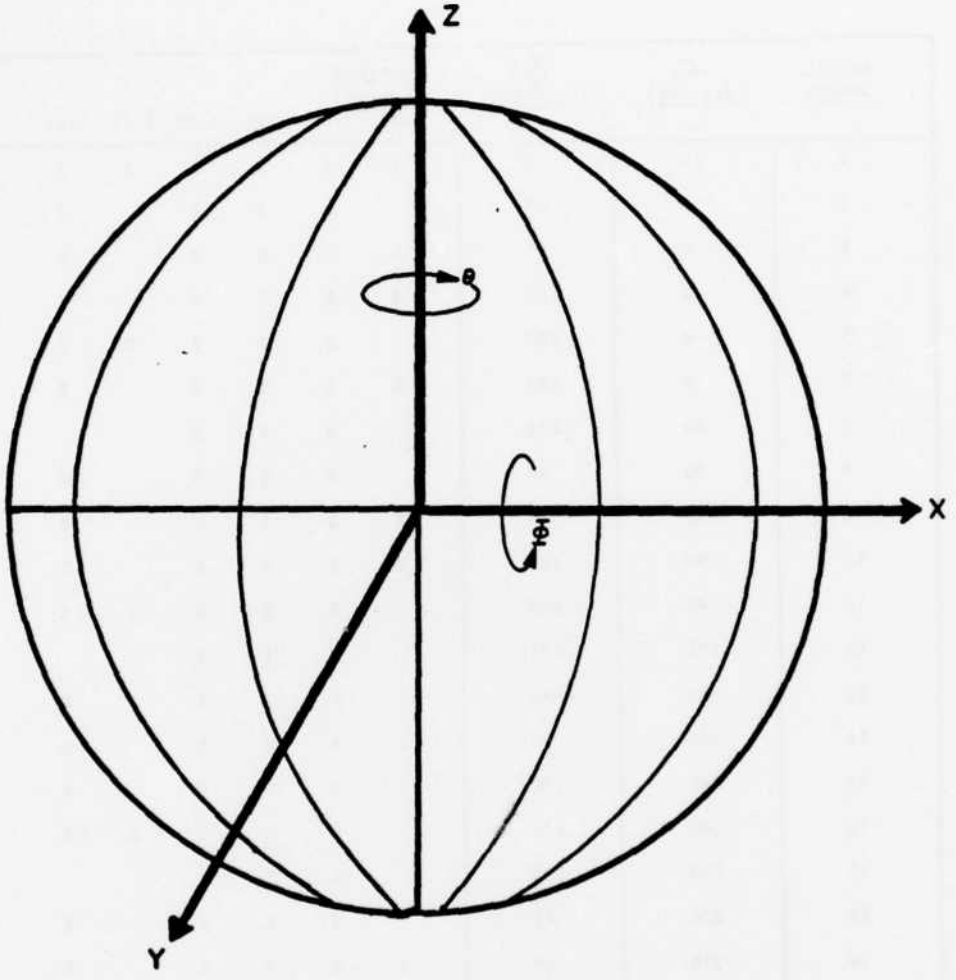

Figure 3. TOA crystal coordinate system.

II. EXPLOSIVE CONSIDERATIONS

The ANFO has been successfully used as the primary explosive for the past 6 years in large-yield field tests. Typically, the explosive is shipped to the site in 22.7 kg (50 lb) bags. These bags are then stacked to construct the standard hemispherically capped cylinders. Some of the bags are opened and the granular ANFO is poured into the voids created when stacking the bags. The total weight of the explosive used is controlled to obtain the desired yield.

The Pre-DIRECT COURSE test did not use the previously mentioned technology. The spherical fiberglass container was used to hold the entire explosive weight. Therefore, the ANFO was able to be shipped in bulk and loaded into the container.

Typically when the bagged charges are completed the total weight and volume is measured, thus, allowing the density to be calculated. The average value of the density from past events is 0.87 g/cc (0.0314 lb/in^3) (Ref. 1). This value takes into consideration the mass of paper, glue and other materials which are not ANFO. On Pre-DIRECT COURSE the fiberglass container was designed around the 0.87 g/cc (0.0314 lb/in^3) density so the volume would contain 20.884×10^3 kg (4.604×10^4 lb). After the loading operation was complete and two days for explosive settling had passed the container was topped off. At this point the charge had a total weight of 20.884×10^3 kg (4.604×10^4 lb) which results in a nominal density of 0.87 g/cc (0.0314 lb/in^3).

1. CHARGE INITIATION

Figure 4 shows a cross section of the charge and associated fiberglass container. In the center of the ANFO sphere is a 30.48 cm (1 ft) diameter, 25.4 kg (56 lb) Octol sphere. Various properties of Octol are: density,

---

1. Swisdak, M. M., "Explosive Material Quality Control for Mill Race," Proceeding of the MILL RACE Preliminary Results Symposium, POR 7073-1, Defense Nuclear Agency, Washington, DC, July 1982.

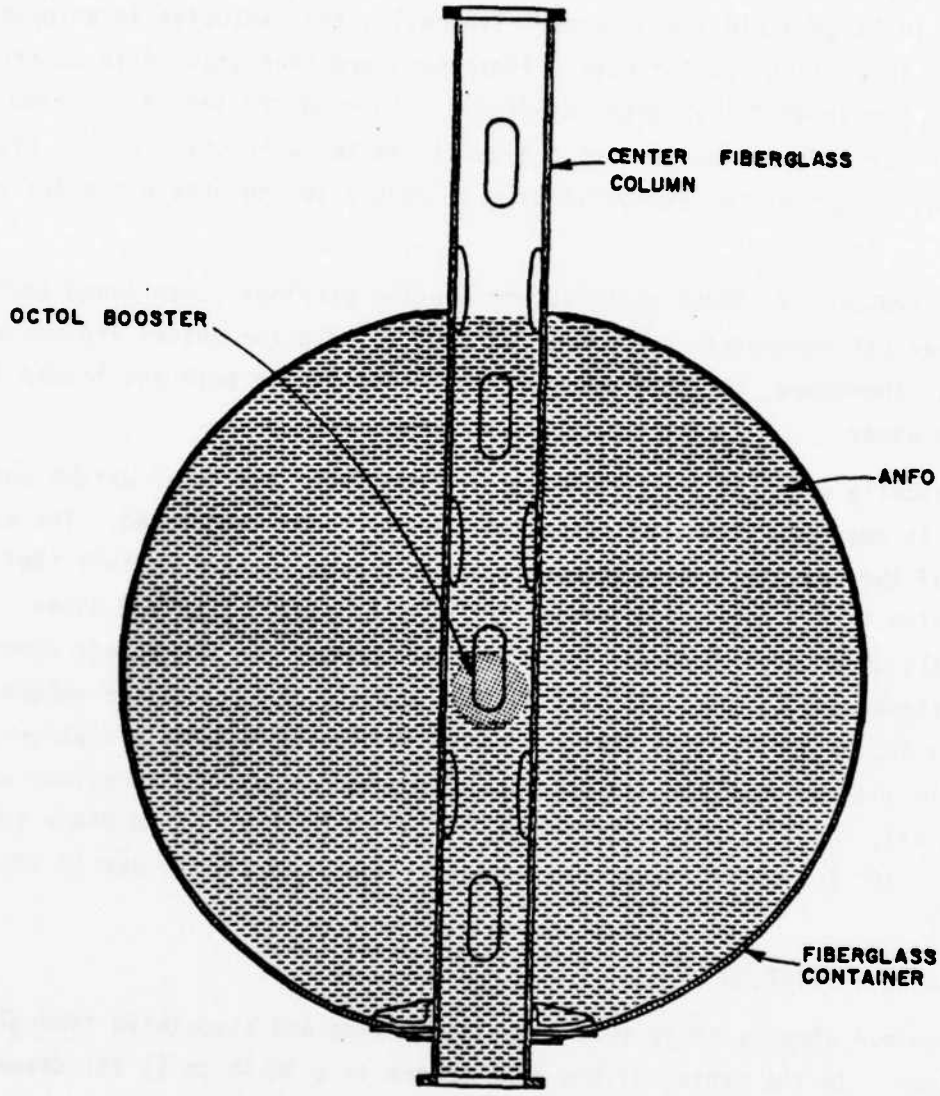

Figure 4. Cutaway view of explosive container and charge.

1.8 g/cc (0.065 lb/in^3); Chapman--Jougnet (C-J) pressure, 31.4 ± 0.69 MPa (4553 ± 100 psi); C-J shock velocity, 8550 ± 29 m/s (28000 ± 95 ft/s); C-J particle velocity, 2040 ± 50 m/s (6690 ± 164 ft/s) (Ref. 2).

The booster was initiated by a cast and machined brass subbooster. The subbooster was initiated by two-7.6 m (25 ft) long flexible confined detonating cords. These cords were initiated by two TC-234 Explosive Burn Wire (EBW) detonators which were connected, by 60.9 m (200 ft) of Reynolds C cable, to the Sandia National Laboratory (SNL) firing unit.* Figure 5 shows a block diagram of the charge initiation system.

This type of charge initiation system would allow placement of the booster, brass subbooster, and confined detonating cords in the ANFO charge during the sphere loading operation. Also, this type of system is the most practical and safest method to use since the sphere would be fully loaded a few days prior to the actual shot day.

The major problem associated with this charge initiation system is the time of true time zero. Time zero can be defined as the actual time the ANFO explosives start to detonate. With this type of system two delays are built into the ANFO detonation (neglecting delays in transmitting through cables). The two delays arise from the time of detonation of the confined detonating cords and the Octol booster. The detonating cord will burn with a velocity of 7315 ± 914 m/s (24000 ± 3000 ft/s).** This can result in a delay of 1.04 ± 0.14 ms for a 7.6 m (25 ft) long fuse. The Octol booster has an average burn velocity of 8381 m/s (27500 ft/s) which can add a delay of 18 μs. Therefore, the total delay between the discharge of the firing unit and the start of the detonation can vary between 0.944 and 1.19 ms.

---

2. Federoff, B. T., Encyclopedia of Explosives and Related Items, PATR-2700, Picatinny Arsenal, Dover, New Jersey, 1972.

*Private communication with M. M. Swisdak (Naval Ordnance Laboratory), January 1983.

**Private communication with K. Bell (New Mexico Engineering Research Institute), December 1982.

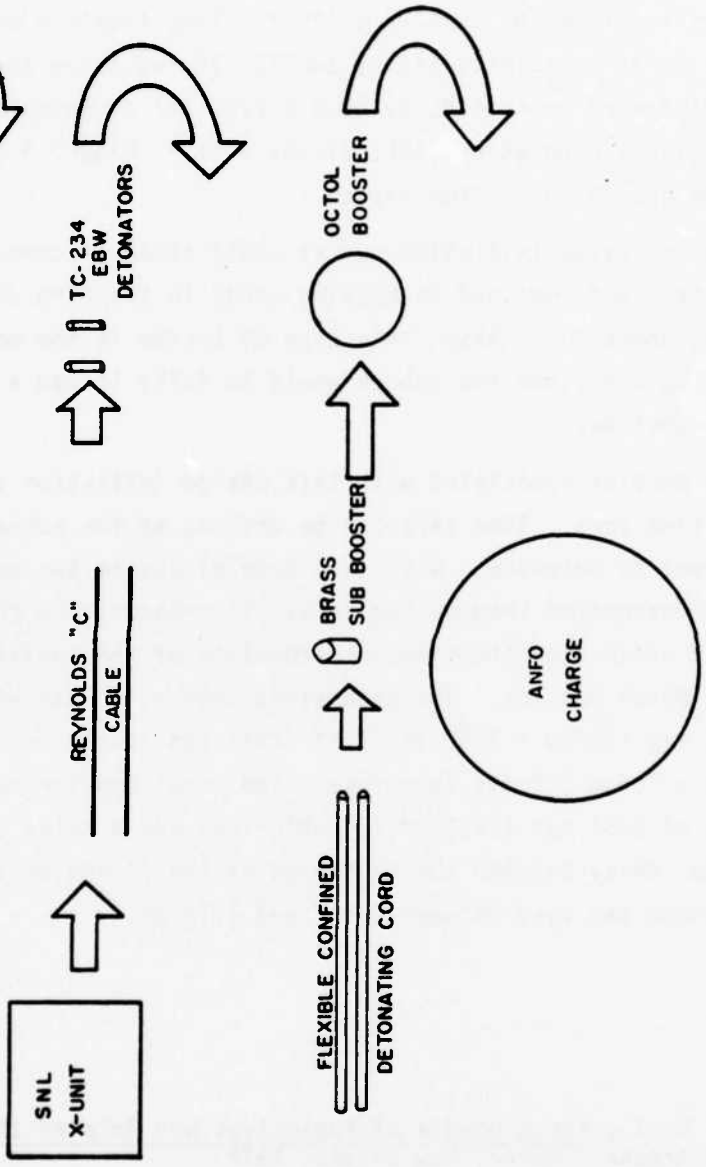

Figure 5. Firing system.

Although this time delay is negligible for most of the experiments, some of the photography experiments need this delay data. Ultrahigh-speed cameras were used on Pre-DIRECT COURSE and for some of them this time delay is twice the order of their total exposure time. Therefore, if the start signal received from the timing and firing van is not adjusted the entire experiment may be unsuccessful.

2. EXPLOSIVE BURN TIME

Since ANFO has been used extensively in recent high yield events the nominal burn rate is fairly well known. If the density of the ANFO is maintained at 0.87 g/cc (0.0314 lb/in^3) and the variation in the fuel oil content is between 4.85 and 7 percent, then the detonation velocity should range between 4199 and 4401 m/s (13,776 and 14,400 ft/s) (Ref. 3).

On Pre-DIRECT COURSE the interior radius of the sphere was 1.77 m (5.81 ft). The Octol booster was 15.24 cm (6 in) in radius, so the total vector length of ANFO is 1.62 m (5.31 ft). Using this distance and the average burn velocities, all of the ANFO would be expected to detonate somewhere between 369 and 387 μs after true time zero.

3. EXPERIMENTAL CRYSTALS

Twenty crystals were placed in a 2.7 by 6 m (8.86 by 19.7 ft) rectangle, 23 m (75.5 ft) from ground zero. The purpose was to investigate various crystal configurations for sensitivity to electromagnetic fields. Such fields have been observed with free detonations aboveground (as opposed to High Explosive Simulation Tests). The configuration of Pre-DIRECT COURSE was thought to be a good candidate for producing a field.

If a plasma is formed and an electrical charge develops which is abruptly grounded, an electromagnetic pulse is radiated (Ref. 4). This pulse can reach the TOAD input sensitivity, and thereby, trigger a measurement before the blast wave arrives.

---

3. Sadwin, L. D. and Swisdak, M. M., Peformance of Multiton AN/FO Detonations, A Summary Report, White Oak, Silver Spring, Maryland, July 1983.

4. Cook, M. A., The Science of High Explosives, Reinhold Book Corp, New York, New York, 1958.

Two regular unterminated crystals were in the matrix for control purposes. Five regular crystals were terminated with 50 Ω, as a means of attenuation. Five crystals were hooded with fine copper mesh with the hood connected to the shield of the coaxial cable, five additional hooded crystals had the hood connected to a ground at the crystal location. These steps were taken to shield the crystals from any electrical field. On two regular crystals, 10 turns of the coaxial pigtail of the gage were wound through a ferrite core to attenuate a current that might be induced in the shield of the coaxial cable and subsequently couple into the center conductor.

III. RESULTS

1. CHARGE INITIATION

After the signal from the timing and firing van was received by the SNL firing unit, two signals were initiated. One signal carried the high amperage to the detonators and the other carried a low voltage to the TOADS forward unit. The signal to the TOADS can be assumed to be void of the time losses associated with signals progressing over thousands of feet of cable (in contrast to the time zero signals used to start cameras). This signal was used in the TOADS to start all of the digital clocks associated with each TOA measurement. For future reference, the time the signal received from the firing unit is used as the absolute zero time.

Measurements 8000 and 8001 were planned to be on the Octol booster. However, after a data review was performed (Appendix A for all raw TOA data) it was deduced that the cables for measurements 8000 and 8002 were crossed. This resulted in an average detonation time measurement of 1173.6 μs of the Octol booster.

This time is relative to the absolute time zero. The relatively long time (> 1 ms) needed to detonate the booster might be questioned. However, as shown previously, a variation between 0.944 and 1.19 ms is possible due to the charge initiation system. Therefore, 1173.6 μs is a valid number to be used as true zero. (This number should be added to all measurements involving time which received a zero time reference from the timing and firing van.)

2. ANFO DETONATION

Table 2 presents the 22 radials of TOA crystals in the ANFO proper. Angle Θ is measured horizontally, and angle Φ is measured (0 through 180 deg) vertically around the center of the sphere. The data are the average detonation velocity calculated from point to point (crystal to crystal). The averages are linear since no local density variations, decelerations, nor accelerations of burning could be accounted for.

Generally, the ANFO appears to have burned 204 m/s faster in the bottom than the top hemisphere. Two factors can be cited for this anomaly. The first is the composition of the prills (pellet made by prilling). When delivered from the manufacturer the prills seemed rather salmon in color

TABLE 2. RADIALLY MEASURED DETONATION VELOCITIES

Φ \ Θ	0°	45°	90°	135°	180°	225°	270°	315°
0°	4132*	-	-	-	-	-	-	-
45°	4198	-	4185	-	4084	-	4568 (Questionable) (Data)	-
90°	4476	-	4434	-	4108	-	4444	-
120°	4518	-	4181	-	4521	-	4481	-
135°	-	4618	-	4522	-	4584	-	4522
150°	4698	-	4379	-	4363	-	4251	-
180°	4155	-	-	-	-	-	-	-

BOTTOM HEMISPHERE

*ALL UNITS IN M/S

and were similar to previous buys. However, many fines were light in mass and resembled wood ash in texture. Some of these fines were blown away during the loading operations, but many were transferred to the fiberglass container. When in the container, the multisized particles were of such geometry and size that the heavier particles could have easily settled to the lower hemisphere of the container. This could have increased the mass of the ANFO in the lower hemisphere when calculated on a volume basis. Therefore, it would be assumed that the detonation velocity would be high due to the higher density because of the natural compaction. The second factor contributing to the higher velocity is similar to the first. After the container was initially loaded, it was allowed to settle for a couple of days. After this period, settlement did occur and a void in the top of the sphere was observed. In the evening prior to shot day, this void was filled to a total weight of 20.884×10^3 kg (46,040 lb). This settlement leads to the assumption that the majority of the ANFO prills repositioning occurs in the lowest, progressing to the upper, portion of the charge. This results in a higher density of ANFO being located in the lower portion of the hemisphere, thus, resulting in a higher detonation velocity. This occurrence has been recorded in prior large high-explosive events at the bottom of the charges. Measurements seem to indicate that the bottom of the charge has a greater detonation velocity than the upward progressing portion of the charge. These factors, considered together, predict that the lower hemisphere will burn faster than the upper hemisphere. Also, some preliminary photographic data indicate that this characteristic was present (Ref. 5). Hopefully, the photographic analysis reports will identify this anomaly and give precise measurements of its magnitude and location.

3. AVERAGE DETONATION VELOCITIES

The TOA crystals placed allow similar radial distance measurements throughout various locations within the charge. The first sphere of crystals was located 0.38 m (1.25 ft) from the center of the charge. The average detonation wave arrival time was 1271.95 μs with a standard deviation of

---

5. Dudziak, W., "High Speed Photograph of Pre-DIRECT COURSE Detonation," presented at Pre-DIRECT COURSE Preliminary Photography Meeting, Field Command, Defense Nuclear Agency, Kirtland AFB, NMex, October 1982.

171.13 μs. The next sphere of crystals was located at 0.76 m (2.5 ft) from the center of the charge. This average detonation wave arrival time was 1306.16 μs with a standard deviation of 21.35 μs. The crystals located at 1.14 m (3.75 ft) from the center of the charge recorded a mean detonation wave arrival time of 1391.78 μs with a standard deviation of 14.29 μs. The next sphere of the charge had crystals located at a radius of 1.52 m (5.0 ft) from the center of the charge. These crystals recorded an average detonation wave arrival of 1457.81 μs with a standard deviation of 57.70 μs. The final sphere of TOA crystals was located on the exterior surface of the fiberglass container. This radius was 1.84 m (6.04 ft) from the center of the charge. These few crystals recorded an average arrival time of 1652.10 μs with a standard deviation of 144.22 μs.

These data follow typical statistical behavior. As the number of observations increases the standard deviation becomes smaller and the average measurements indicate the norm. Therefore, it can be assumed that the mid-distance measurements are the most accurate and should be used for velocity measurements.

4. STRUCTURAL DESIGN EFFECTS

Upon initial observation of the fiberglass component design, it would be assumed that the design would affect the propagation of the detonation wave. The holes in the interior support column and the column itself would appear to have a tremendous effect on the spherically diverging detonation wave. The column would tend to act as a shock tube allowing the wave to expand in two directions instead of three. The holes would allow point sources of charge initiation assuming that the fiberglass burns much slower than the ANFO. However, from the data obtained, the effect of the design is not as drastic as assumed.

The fiberglass column did not act as a shock tube. In fact, the two radials extending through the center of the tube recorded some of the lowest detonation velocities in the entire sphere (4133 and 4154 m/s) (13,560 and 13,630 ft/s). If the column initiated as a shock tube, a majority of the energy was absorbed into the fiberglass or lost through the holes throughout the column.

The unique construction of the center column did not seem to have as dramatic an effect as anticipated. The Swiss-cheese design was chosen to allow easy filling of the column with ANFO and also to minimize detonation problems. Figure 6 shows a view of the center column and some of the TOA crystals located on the 0.38 m (1.25 ft) radius. The sketch is in three-dimensional perspective, therefore, the crystals are represented as points on an imaginary sphere having a radius of 0.38 m (1.25 ft). Measurements 8000 and 8006 are in the interior of the column. The number in parenthesis is the TOA of the detonation wave at that location. As can be seen, the detonation wave did not reach each of the points at the same time. In fact, the crystals in the interior of the column were triggered later than most of the other crystals. By careful study of this figure it can be noted that measurements 8010 and 8015 are 180 deg apart. Also, there is a hole in the center column between the booster and measurement 8010, whereas there is the wall of the fiberglass column between the booster and measurement 8015. Only 1 μs separates the recorded TOA at these locations, which seems to indicate that the column had little or no effect on the detonation wave. The same result is obtained, if similar collocated measurements are studied.

5. LARGE BURN IRREGULARITIES

The ANFO events are usually characterized by some degree of burn irregularities or jetting. This characteristic can be caused by nonuniform explosive properties, detonator placement, and localized hot spots. The ultrahigh-speed photography used on Pre-DIRECT COURSE indicated that the bottom hemisphere broke out first at approximately Θ = 0 deg and Φ = 150 deg. The next frames indicate a jetting on the top near the fiberglass column and, finally, the entire sphere was illuminated. The photography also indicates that the solid fiberglass seams connecting the fiberglass and balsa wood panels (which make up the container) retard the fireball. However, the photography does not indicate any type of disturbance to the detonation wave.

Table 2, which shows the average radial detonation velocities at selected locations, indicates that a fast burn did occur in the Θ = 0 deg to 45 deg and Φ = 120 deg to 150 deg region. These data would then substantiate the photographic data. A possible cause for this irregularity, although impossible to verify, is that the location for the access port and ANFO loading port is at Θ = 90 deg. This particular location may account for uneven compaction of the ANFO.

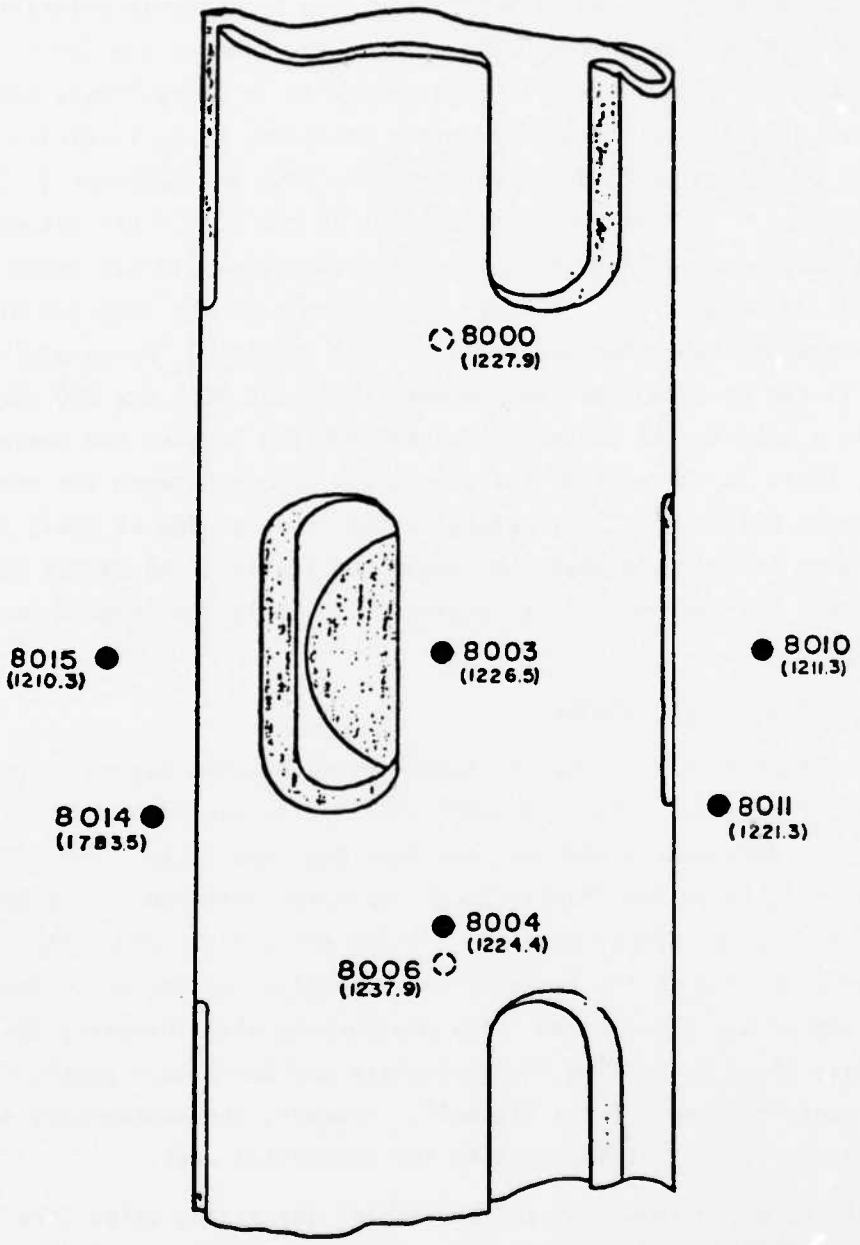

Figure 6. Close-up of center column and TOA crystals.

Another region which shows large detonation velocities is at Θ = 135 deg for all angles of Φ. These locations exhibit velocities near an average of 100 m/s (328 ft/s) above those velocities from nearby radials. There is no known rationale for this characteristic. However, a phenomenon similar to this was seen in a calculation performed by S-Cubed.*

With the exceptions of the aforementioned radials the detonation wave progressed symmetrically. The average detonation velocity for the top hemisphere was 4150 m/s (13,615 ft/s) and for the bottom hemisphere 4437 m/s (14,560 ft/s). These values fall within the range (4200 to 4400 m/s) (13,780 to 14,436 ft/s) observed on previous ANFO events.

6. CONTAINER BREAKOUT

Four crystals placed on the interior surface of the container recorded extremely close data. The average arrival time was 1536 ± 7.3 μs. This can also be translated as the average amount of time needed to detonate all of the ANFO (time zero must be accounted for).

Eighteen crystals were located on the exterior of the container and seven failed. The majority of the crystals which failed were located on this surface. Assessing the bad data, it was found that all four of the crystals located on Θ = 270 and all angles of Φ failed. This would be indicative of a jet (as from the Θ = 150 deg, Φ 135 deg region) cutting the cables prior to crystal triggering. The good data indicate that the exterior crystals were triggered at approximately 1579 μs.

Studying two crystals (measurement numbers 8005 and 8086), which are separated by only the fiberglass seam thickness, it can be deduced that the TOA between the two crystals is only 13.2 μs. The exterior crystals also indicate that a premature breakout of the charge was located at the Θ = 0 deg, Φ = 150 deg region. An important final note is that all of the crystals located on the container (interior and exterior) were located on the fiberglass seams and not on any panel.

---

*Kennedy, L., "HULL Code Predictions of Pre-DIRECT COURSE," presented at Pre-DIRECT COURSE Preliminary Photography Meeting, Field Command, Defense Nuclear Agency, Kirtland AFB, NMex, October 1982.

7. EXPERIMENTAL CRYSTALS

Pre-DIRECT COURSE did not produce enough electromagnetic radiation to trigger the regular unattenuated crystals. It is believed that the tower grounding system arrested the majority of the electrical discharge from the detonation. This in turn would not allow the field to build up and then discharge.

Figure 7 shows a plot of the data measured by the experimental crystals. The data indicate that the good measurements are within the expectations of the blast wave arrival.

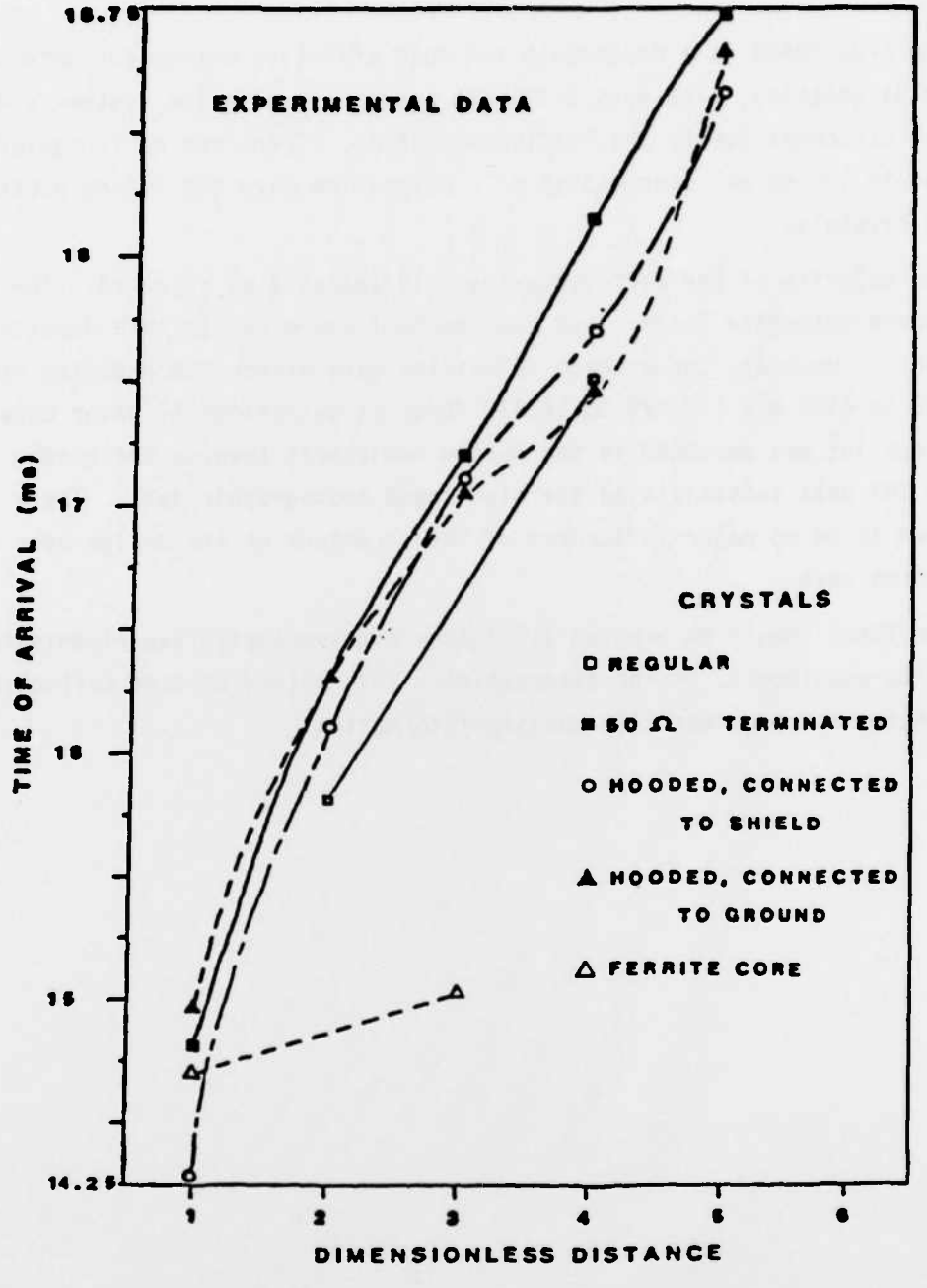

Figure 7. Experimental TOA results.

IV. CONCLUSIONS

The AFWL TOADS is a dependable and cost effective method for determining charge diagnostics. The most difficult aspect of using the system is exact crystal placement due to the loading operation. There are no irregularities induced in the normal progression of a detonation wave due to the presence of TOA crystals.

The majority of the ANFO explosives did detonate as expected. The bottom hemisphere detonated faster than the top hemisphere due to ANFO density gradients. However, the average velocities were within the expected range of 4200 to 4400 m/s (13,780 to 14,436 ft/s) as determined by prior data. One large jet was measured in the bottom hemisphere towards the north. All of the TOA data substantiated the high-speed photographic data. There appeared to be no major influences of the structure or its design upon the detonation wave.

The TOADS should be used on all future high-explosive experiments to act as, or to supplement, charge diagnostics. This method of data collection is inexpensive and provides high-quality information.

APPENDIX A

This appendix contains the raw data received from the TOA crystals in and on the container. Also included are general comments. Refer to Figure 3 for explanation of angles and coordinate system.

TOA MEASUREMENT NUMBER	COMMENTS	θ RELATIVE TO TOWER (deg)	φ RELATIVE TO TOWER (deg)	ε RELATIVE TO TEST BED (deg)	R FROM CENTER OF SPHERE (ft)		TIME OF ARRIVAL (μs)
8000	should be 8002	ON	BOOSTER		0.5		1227.9
8001		ON	BOOSTER		0.5		1166.7
8002	should be 8000	0	0	15	1.25		1180.5
8003		0	90	15	1.25		1226.5
8004		0	120	15	1.25		1224.4
8006		0	180	15	1.25		1237.9
8008		180	120	195	1.25		1218.1
8009		180	90	195	1.25		1205.7
8010		270	90	285	1.25		1211.3
8011		270	120	285	1.25		1221.3
8014	Questionable data	90	120	105	1.25		1783.5
8015		90	90	105	1.25		1210.3
8016		315	135	330	2.5		1311.9
8017		45	135	60	2.5		1306.5
8018		135	135	150	2.5		1290.7
8019		225	135	240	2.5		1226.5
8020		0	0	15	2.5		1259.3
8021	Cable slap	270	45	285	2.5		6384.3

TOA MEASUREMENT NUMBER	COMMENTS	θ RELATIVE TO TOWER (deg)	ϕ RELATIVE TO TOWER (deg)	ϵ RELATIVE TO TEST BED (deg)	R FROM CENTER OF SPHERE (ft)		TIME OF ARRIVAL (μs)
8022		0	45	15	2.5		1311.3
8023		90	45	105	2.5		1305.1
8024		180	45	195	2.5		1308.5
8025		0	90	15	2.5		1318.5
8026		0	120	15	2.5		1314.5
8027		0	150	15	2.5		1313.7
8028		0	180	15	2.5		1303.9
8029		180	150	195	2.5		1308.3
8030		180	120	195	2.5		1310.5
8031		180	90	195	2.5		1298.9
8032		270	90	285	2.5		1305.5
8033		270	120	285	2.5		1319.7
8034		270	150	285	2.5		1310.3
8035		90	150	105	2.5		1323.1
8036		90	120	105	2.5		1314.3
8037		90	90	105	2.5		1305.3
8038		315	135	330	3.75		1398.7
8039		45	135	60	3.75		1389.9

TOA MEASUREMENT NUMBER	COMMENTS	θ RELATIVE TO TOWER (deg)	♦ RELATIVE TO TOWER (deg)	ε RELATIVE TO TEST BED (deg)	R FROM CENTER OF SPHERE (ft)		TIME OF ARRIVAL (μs)
8040		135	135	150	3.75		1377.5
8041		225	135	240	3.75		1386.3
8042		0	0	15	3.75		1347.9
8043		270	45	285	3.75		1415.7
8044		0	45	15	3.75		1399.3
8045	Did not trigger	90	45	105	3.75		11.7
8046		180	45	195	3.75		1395.1
8047		0	90	15	3.75		1401.3
8048		0	120	15	3.75		1396.5
8049		0	150	15	3.75		1396.1
8050		0	180	15	3.75		1410.7
8051		180	150	195	3.75		1390.5
8052		180	120	195	3.75		1393.1
8053		180	90	195	3.75		1382.1
8054		270	90	285	3.75		1390.7
8055		270	120	285	3.75		1399.9
8056	Did not trigger	270	150	285	3.75		0.9
8057		90	150	105	3.75		1387.7

TOA MEASUREMENT NUMBER	COMMENTS	θ RELATIVE TO TOWER (deg)	ϕ RELATIVE TO TOWER (deg)	ε RELATIVE TO TEST BEO (deg)	R FROM CENTER OF SPHERE (ft)		TIME OF ARRIVAL (μs)
8058		90	120	105	3.75		1394.3
8059		90	90	105	3.75		1390.1
8060		315	135	330	5.0		1480.5
8061		45	135	60	5.0		1470.7
8062		135	135	150	5.0		1459.3
8063		225	135	240	5.0		1467.7
8064		0	0	15	5.0		1434.3
8065		270	45	285	5.0		1499.1
8066		0	45	15	5.0		1487.1
8067		90	45	105	5.0		1480.7
8068		180	45	195	5.0		1481.5
8069	Questionable data	0	90	15	5.0		1229.7
8070		0	120	15	5.0		1478.7
8071		0	150	15	5.0		1475.9
8072		0	180	15	5.0		1496.7
8073		180	150	195	5.0		1470.5
8074		180	120	195	5.0		1472.1
8075		180	90	195	5.0		1465.3

TOA MEASUREMENT NUMBER	COMMENTS	θ RELATIVE TO TOWER (deg)	♦ RELATIVE TO TOWER (deg)	ε RELATIVE TO TEST BED (deg)	R FROM CENTER OF SPHERE (ft)		TIME OF ARRIVAL (μs)
8076		270	90	285	5.0		1474.1
8077		270	120	285	5.0		1479.3
8078		270	150	285	5.0		1348.1
8079		90	150	105	5.0		1469.7
8080		90	120	105	5.0		1476.9
8081		90	90	105	5.0		1473.9
8005	On interior surface of container	0	150	15	5.83		1535.7
8007	On interior surface of container	180	150	195	5.83		1535.5
8012	On interior surface of container	270	150	285	5.83		1543.3
8013	On interior surface of container	90	150	105	5.83		1529.5
8082	On exterior of container	0	90	15	6.04		1554.5
8083	Cable slap	270	90	285	6.04		5917.3
8084	On exterior of container	0	120	15	6.04		1550.5
8085	bad crystal	270	120	285	6.04		-------
8086	On exterior of container	0	150	15	6.04		1548.9
8087	Cable slap	270	150	285	6.04		4187.9
8088	bad crystal	0	180	15	6.04		-------
8089	Questionable Data	180	150	195	6.04		1940.9

TOA MEASUREMENT NUMBER	COMMENTS	θ RELATIVE TO TOWER (deg)	♦ RELATIVE TO TOWER (deg)	ε RELATIVE TO TEST BED (deg)	R FROM CENTER OF SPHERE (ft)		TIME OF ARRIVAL (μs)
8090	On exterior of container	90	150	105	6.04		1581.7
8091	Questionable Data	180	120	195	6.04		1853.1
8092	On exterior of container	90	120	105	6.04		1581.7
8093	On exterior of container	180	90	195	6.04		1605.5
8094	On exterior of container	90	90	105	6.04		1544.9
8095	Cable alap	270	45	285	6.04		2571.3
8096	On exterior of container	0	45	15	6.04		1572.1
8097	On exterior of container	0	0	15	6.04		1577.5
8098	On exterior of container	90	45	105	6.04		1575.9
8099	On exterior of container	180	45	195	6.04		1658.1

APPENDIX B

This appendix contains raw data from the experimental crystals. The tables describe each crystal and modification, the distance from ground zero and the time of shock arrival.

MEASUREMENT NUMBER	DESCRIPTION		ELEVATION	DISTANCE FROM GROUND ZERO (ft)		COMMENTS	TIME OF ARRIVAL (μs)
8101	hooded crystal, w/hood connected to ground at location		0	75.5			14960
8102	hooded crystal, w/hood connected to cable shield		0	75.5			14286
8103	Regular Crystal 50 ohm terminated		0	75.5			14829
8104	Regular Crystal, ten turns thru Ferrite Core		0	75.5			14719
8105	Same as 8102		0	80.5			16118
8106	Same as 8103		0	80.5		Questionable	1621.9
8107	Regular Crystal		0	80.5			15855
8108	Same as 8101		0	80.5			16256
8109	Same as 8103		0	85.5			17212
8110	Same as 8104		0	85.5		Questionable	15028
8111	Same as 8101		0	85.5			17109
8112	Same as 8102		0	85.5			17121
8113	Same as 8107		0	90.5			17510
8114	Same as 8101		0	90.5			17474
8115	Same as 8102		0	90.5			17709
8116	Same as 8103		0	90.5			18188
8117	Same as 8101		0	95.5			18829
8118	Same as 8102		0	95.5			18665

MEASUREMENT NUMBER	DESCRIPTION		ELEVATION	DISTANCE FROM GROUND ZERO (ft)		COMMENTS	TIME OF ARRIVAL (μs)
8119	Same as 8103		0	95.5			18994
8120	Same as 8107		0	95.5		No Data	-----


DATE
ILME